Available online at www.sciencedirect.com
ScienceDirect
Ceramics International 37 (2011) 3609–3616
CERAMICS INTERNATIONAL
www.elsevier.com/locate/ceramint

Synthesis and characterization of praseodymium-containing $ZrSiO_4$ solid solutions from gels

N. Montoya, G. Herrera, J. Alarcón *

Department of Inorganic Chemistry, University of Valencia, Calle Dr. Moliner 50, 46100 Burjasot (Valencia), Spain

Received 11 March 2011; received in revised form 6 June 2011; accepted 9 June 2011
Available online 15 June 2011

Abstract

The preparation and characterization of a series of praseodymium–zircon solid solution (Pr_x–$ZrSiO_4$) materials with increasing nominal amounts of Pr is reported. Pr-doped zircon gels were prepared by gelling mixtures of zirconium n-propoxide, praseodymium acetylacetonate and tetraethylorthosilicate, and annealed over the range of temperature up to the formation of Pr–zircon solid solutions. The reaction sequence was followed by X-ray powder diffraction (XRD), ultraviolet–visible diffuse reflectance (DR) and infrared spectroscopy (IR). The first crystalline phase detected on annealing gels was a tetragonal praseodymium-containing ZrO_2 phase (t-Pr–ZrO_2). On further annealing, the subsequent transformation to the monoclinic form (m-Pr–ZrO_2) took place. The formation of final Pr–$ZrSiO_4$ solid solutions occurred by the reaction between m-Pr–ZrO_2 and amorphous silica phase. The mechanism of solid solution formation inferred from energy dispersive X-ray microanalysis (SEM/EDX) data, variation of lattice parameters and DR of final Pr–$ZrSiO_4$ solid solutions involved the replacement of Zr^{4+} by Pr^{4+} in dodecahedral sites of the zircon structure. DR revealed that a relatively small amount of Pr^{3+} was still present in final Pr-containing $ZrSiO_4$ products. The estimated solubility of praseodymium in the zircon was around 0.067 mol of praseodymium per mol of zircon (~11.5 wt% as Pr_2O_3). This study opens new perspectives to the development of more ecological zircon-based ceramic pigmenting systems by using mineralizer-free sol–gel synthetic techniques.

Keywords: Ceramic pigments; Solid solutions; Zircon; Zirconia; Sol–gel; Pr^{4+}

1. Introduction

Pigmenting systems based on the zircon structure have been used industrially for, at least, five decades ago. These materials accomplish the requirements (or properties) regarding with chemical stability at high temperatures in corrosive glasses (or glazes) and high tinctorial strength. One of such pigments is the so-called yellow praseodymium zircon, in which the praseodymium cation gives rise to the yellow colour [1].

Since the first studies on this pigmenting system in the 1960s, several authors have been concerned with technical aspects in order to improve its industrial manufacture [2,3]. Regarding with fundamental knowledge of this pigmenting system, it is assumed that its yellow colour is due to the formation of a zircon-based solid solution, in which the praseodymium cation occupy structural sites in the zircon lattice [4]. Recently several authors have searched different points concerning structural and chemical features of this pigmenting system. Ocaña et al. studied the valence and localization of the praseodymium chemical species in the zircon matrix of a composition of Pr-doped zircon powder obtained by conventional reaction of the metal oxides and mineralizers or fluxing agents. From XRD and XAS (XANES and EXAFS) spectroscopy results, they concluded that Pr cation was in tetravalent state (Pr^{4+}) in the formed Pr–$ZrSiO_4$ solid solution replacing Zr^{4+} cations in triangular dodecahedral sites [5,6]. Badenes et al. prepared Pr–zircon specimens by using different synthetic procedures with and without mineralizer [7]. Their results concluded that final Pr–$ZrSiO_4$ seems to have a mixed nature of solid solution and encapsulated pigment, coexisting Pr^{4+} and Pr^{3+} in each one of the final pigmenting components. Del Nero et al. prepared Pr–zircon specimens by sol–gel techniques and containing different mineralizers [8]. The study of samples by visible-near infrared diffuse reflectance spectroscopy evidenced the presence of Pr^{3+} in final Pr–$ZrSiO_4$. Kar et al. in a recent study on the processing

* Corresponding author. Tel.: +34 96 3544584; fax: +34 96 3544322.
E-mail address: javier.alarcon@uv.es (J. Alarcón).

0272-8842/$36.00
doi:10.1016/j.ceramint.2011.06.019

and characterization of this pigmenting system stated that the intense yellow coloration obtained from specimens prepared with mineralizer by solid state synthesis method, was due to the presence of Pr^{3+} in dodecahedral sites in the zircon lattice [9].

Despite the results reported in the literature, it is evident that some controversial on many fundamental characteristics of Pr–zircon system still remain and more fundamental knowledge on the nature of this pigmenting system is required, in order not only to improve its technical manufacturing without using mineralizers but also to contribute to enlighten some fundamental aspects of Pr–$ZrSiO_4$ solid solution particulated materials. Thus, some of the particular characteristics that should be searched in this pigmenting system would be: (a) to demonstrate its nature as solid solution by proving the lattice parameter variation on increasing the praseodymium content inside the zircon lattice in a series of samples; (b) to estimate the limit of solubility of Pr in the zircon host lattice, and; (c) to elucidate both the site distribution and the oxidation state of Pr cations in the zircon structure. In order to obtain more conclusive results on those features of Pr–$ZrSiO_4$, synthetic procedures allowing the control of the reaction kinetics at the different stages over the temperature range up to formation of zircon must be used.

It is to note that fundamental knowledge of these monophasic Pr–zircon materials could allow extending their potential applications to other industry fields, such as chemical sensing, as it has been proved recently in V–zircon pigmenting system [10,11].

The advantages of sol–gel synthesis of transient metastable and/or final monophasic solid products have been demonstrated for years ago. Thus, in a previous study on V–zircon pigmenting system [12,13], these techniques allowed the preparation of monophasic final products from a series of mineralizer-free gel precursors, with increasing amounts of vanadium as dopant, carefully annealed at different temperatures.

The main objective of the present contribution is therefore to gain fundamental knowledge on the praseodymium–zircon solid solution system. The annealing of mineralizer-free gel precursors, with nominal compositions Pr_x–$ZrSiO_4$ ($0 \leq x \leq 0.15$), over the range of temperature up to the zircon-based solid solution formation, will allow both the control of reactivity and to elucidate the structural and chemical changes through the whole process leading to Pr–$ZrSiO_4$ materials. Also, the distribution and the chemical state of the praseodymium cation at the different steps will be investigated.

2. Experimental procedure

2.1. Preparation of gel samples

Precursor gels with compositions Pr_x–$ZrSiO_4$, with $x = 0$, 0.01, 0.02, 0.04, 0.05, 0.06, 0.07, 0.08, 0.1 and 0.15, were prepared by the following procedure:

The required amount of zirconium n-propoxide (ZnP, $Zr(OC_3H_7)_4$) from Merck & Co.), to prepare around 2 grams of final doped zircon, was dissolved in a solution of 1-propanol (n-PrOH), and acetylacetone (acac, $C_5H_8O_2$, Merck & Co.). The role of the acac was to slow down the hydrolysis and condensation processes. This first step in the preparation of Pr-doped zircon gels was carried out in a dry atmosphere. Then, the proper amount of Pr, as praseodymium acetylacetonate ($Pr(acac)_3$, $PrC_{15}H_{24}O_6$, Merck & Co.) was added to the zirconium-containing solution. Subsequently, the stoichiometric contents of tetraethylorthosilicate (TEOS, $Si(OC_2H_5)_4$ from Merck & Co.) and H_2O were added to the solution. The final mixture was put into a closed polyethylene bottle and kept at 60 °C for 24 h. Yellowness gels were obtained for all compositions. The ZnP:n-PrOH:acac:TEOS:H_2O molar ratios were 1:8:1:1:5.5 for all the prepared gels.

The homogeneous gels were dried first at room temperature for 2 days and finally at 110 °C for 24 h. Dried gel precursors were annealed over the range of temperatures between 400 °C and 1600 °C for different times.

2.2. Characterization of samples

Chemical and structural evolutions of dried gels and crystalline specimens were examined using several techniques.

Infrared absorption spectra (Model 320 Avatar, Nicolet) were obtained in the range 2000–400 cm^{-1} using the KBr pellet method.

X-ray diffraction analysis (Model AXS D-5005, Bruker) was performed using a graphite monochromatic CuK_α radiation. The diffractometer had two 1° divergence slits, the scatter and receiving slits being 1° and 0.05°, respectively. The diffractograms were run with a step size of 0.02 $2\theta^\circ$ and a counting time of 10 s. The determination of the lattice constants of zircon was made using the DICVOL indexing program.

Energy-dispersive X-ray analysis was performed using a scanning electron microscope (Model XL30 ESEM, Philips) operated at 20 kV. This instrument is equipped with an energy dispersive X-ray spectrometer (Model XL30 132-2.5, EDAX). Two types of analysis were performed. The first type intended to obtain the overall analysis of the whole sample in annealed gels at 1600 °C. These analyses were obtained by scanning the electron beam across a large area of the specimens (100 μm × 100 μm), giving the averaged composition of the area displayed. The second type of analysis involved the determination of the composition of final praseodymium–zircon solid solution phases. It was carried out by spot analysis, in which the electron beam was stopped and positioned on the point to be analyzed, as selected on the scanning electron microscope screen. Quantitative analyses of specimens were made using the EDAX GENESIS program with ZAF correction procedures and the default standards.

UV–vis diffuse reflectance (DR) spectra of the specimens (Model V-670, Jasco) were obtained using the diffuse reflectance technique in the range of 200–2500 nm. $L^*a^*b^*$ parameters of representative specimens were measured using the above Jasco spectrophotometer using a standard lighting C, following the CIE-$L^*a^*b^*$ colorimetric method recommended by the CIE (Commision Internationale de ÍEclairage). In this colour system, L^* is the colour lightness ($L^* = 0$ for black and 100 for white), a^* is the green (−)/red (+) axis, and b^* is blue (−)/yellow (+) axis.

3. Results and discussion

3.1. Formation of Pr–$ZrSiO_4$ solid solutions

In this point we intend to know the structural transformations and the experimental conditions required to obtain Pr_x–$ZrSiO_4$ solid solutions from mineralizer-free gels with different praseodymium loadings. Also, is aimed to obtain information on the praseodymium location and chemical state at the different steps in the whole process of Pr–zircon solid solution formation.

3.1.1. Structure of gel precursors

The infrared spectra of the dried gels Pr_x–$ZrSiO_4$ for compositions $x = 0$ and 0.1, shown as representatives, are displayed in Fig. 1. Bands at around 1150 and 1050 cm^{-1} are attributed to asymmetric stretching vibrations of Si–O–Si bonds [14–16]. Also associated with Si–O bonds appear bands at 870 and 460 cm^{-1}, ascribed to bending modes of O–Si–O and Si–O–Si bonds [15,16]. Other bands at 1630, 1410 and 620 cm^{-1} associated with OH groups, C–H bonds and Zr–O bonds in the ZrO_8 group, respectively, are also observed in the dried gel spectra series [17,18]. According to IR results, there is not evidence of formation of a three-dimensional Si–O–Zr network in these gel precursors but both silica and zirconia components are separated forming individual domains in a diphasic system.

3.1.2. Structural changes from gels to Pr–ZrO_2 solid solutions

The evolution of crystalline phases in Pr_x–$ZrSiO_4$ as a function of the annealing temperature in gels with increasing praseodymium content is summarized in Table 1. As can be seen, three main crystalline phases can be distinguished during the evolution from gels: the first one is a phase with structure of tetragonal ZrO_2; the second is a monoclinic ZrO_2 phase brought out by phase transformation of the tetragonal; and finally the Pr-containing zircon yielded by reaction between monoclinic ZrO_2 and amorphous silica. The formation of metastable transient tetragonal and monoclinic ZrO_2 crystalline phases on annealing gels, with increasing praseodymium nominal loadings, at different temperatures, is shown in Figs. 2 and 3, respectively. As can be seen those materials based either on tetragonal or monoclinic Pr-containing zirconia in presence of an amorphous silica network can be quasi-selectively prepared in the ternary system Pr_2O_3–ZrO_2–SiO_2.

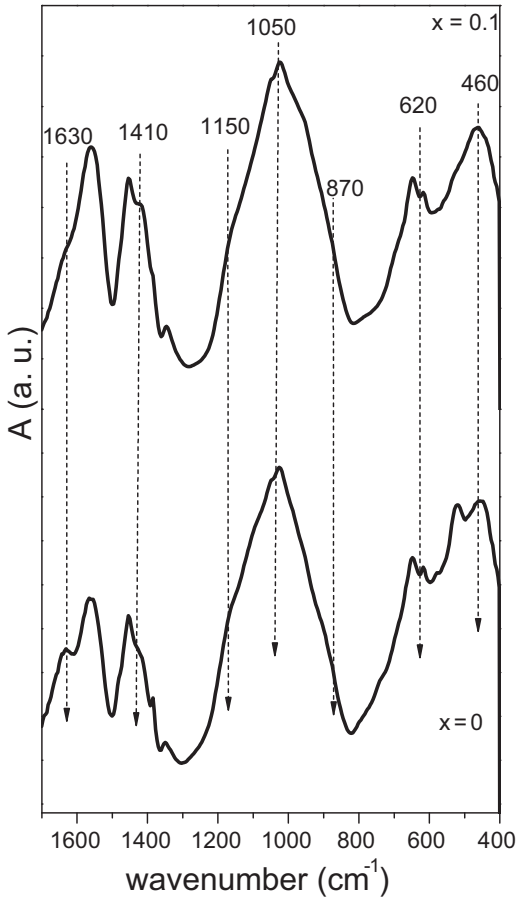

Fig. 1. Infrared spectra of dried gels Pr_x–$ZrSiO_4$: (a) $x = 0$; (b) $x = 0.1$.

As can be inferred from Table 1, the temperature of zircon-based solid solution formation is slightly dependent on the nominal amount of praseodymium. The required temperature for complete zircon development goes down over the range of compositions from undoped $ZrSiO_4$, i.e. $x = 0$, to $Pr_{0.07}$–$ZrSiO_4$. For higher loadings of praseodymium than $x = 0.7$ the temperature raise with increasing the amount of Pr. This behaviour is different to the one reported for vanadium as dopant of zircon, in which the temperature of zircon formation experiences a large reduction as the vanadium content goes up [12]. In general, for all Pr-containing gels, the formation of tetragonal ZrO_2 takes place at around 1000 °C and the transformation to the monoclinic form starts at around 1250 °C. On contrast the temperature of reaction between

Table 1
Evolution of crystalline phases in Pr–$ZrSiO_4$ system at different temperatures.

x	Temperature/holding time			
	1100 °C/3 h	1200 °C/3 h	1400 °C/3 h	1600 °C/24 h
0	t-ZrO_2	t-ZrO_2 + m-ZrO_2(vw)	$ZrSiO_4$(vw) + t-ZrO_2(w) + m-ZrO_2(s)	$ZrSiO_4$ + t-ZrO_2(vw)
0.02	t-ZrO_2	t-ZrO_2 + m-ZrO_2(vw)	m-ZrO_2(vw) + t-ZrO_2(w) + $ZrSiO_4$(s)	$ZrSiO_4$ + t-ZrO_2(vw)
0.05	t-ZrO_2	m-ZrO_2 + t-ZrO_2(s)	m-ZrO_2(m) + t-ZrO_2(m) + $ZrSiO_4$(s)	$ZrSiO_4$ + t-ZrO_2(vw) + m-ZrO_2(vw)
0.07	t-ZrO_2	m-ZrO_2 + t-ZrO_2(s)	m-ZrO_2(m) + t-ZrO_2(m) + $ZrSiO_4$(s)	$ZrSiO_4$ + t-ZrO_2(vw) + m-ZrO_2(vw)
0.1	t-ZrO_2	m-ZrO_2 + t-ZrO_2(s)	$ZrSiO_4$(m) + t-ZrO_2(w) + m-ZrO_2(s)	$ZrSiO_4$ + $Pr_2Si_2O_7$(vw) + t-ZrO_2(vw)

vw, very weak; w, weak; m, medium; s, strong.

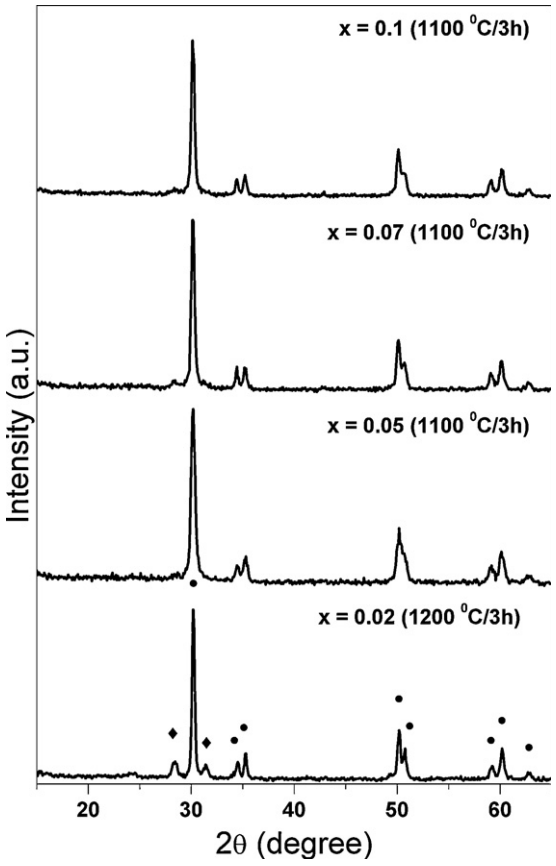

Fig. 2. X-ray diffraction patterns of dried gels Pr_x–$ZrSiO_4$ annealed at 1100 °C or 1200 °C (◆ is monoclinic zirconia and • is tetragonal zirconia).

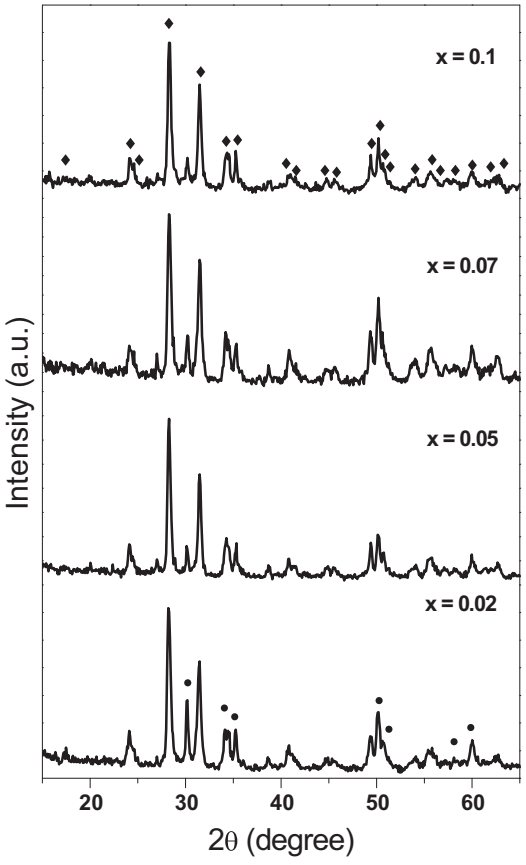

Fig. 3. X-ray diffraction patterns of dried gels Pr_x–$ZrSiO_4$ annealed at 1300 °C/3 h (◆ is monoclinic zirconia and • is tetragonal zirconia).

monoclinic ZrO_2 and amorphous silica phases to yield zircon crystalline phase increases on raising the amount of nominal Pr over $x = 0.07$ in the starting gels. Thus, while for specimen with $x = 0.02$ the formation of Pr–$ZrSiO_4$ is almost complete at 1400 °C for $x = 0.1$ are required even higher temperatures than 1500 °C.

An interesting point to be considered before the formation of crystalline phase with zircon structure is to evaluate both the chemical state and the structural location of silicon and praseodymium at the first reaction stage, i.e. on annealing gels at low temperatures. As at temperatures below the crystallization of tetragonal zirconia is not detected the formation of any crystalline phase containing silicon, it can be inferred that the silica component is present at this stage as amorphous silica. With regard to the praseodymium location and chemical state at low temperature, it is difficult to search because it is a minor component. However, it is possible to obtain information on these interesting issues from X-ray powder diffraction and UV–vis diffuse reflectance results. The first significant structural change on annealing gels is the crystallization of a phase with structure of tetragonal zirconia. At this stage, it seems obvious that the praseodymium cations must be associated with either the zirconia crystalline phase or the amorphous silica. In order to check the second hypothesis, i.e. the possible dissolution of praseodymium in the amorphous silica, a mixture of composition 0.07 $Pr(acac)_3$·TEOS was hydrolysed and after drying, thermally treated at 1000 °C for 3 h. As can be seen in Fig. 4, in which the DR spectra of the specimens $Pr_{0.02}$–$ZrSiO_4$, $Pr_{0.05}$–$ZrSiO_4$, $Pr_{0.07}$–$ZrSiO_4$, $Pr_{0.1}$–$ZrSiO_4$ and $Pr_{0.07}$–SiO_2 heated at 1100 °C/3 h are displayed, the spectra of those specimens, which are made up of tetragonal zirconia–amorphous silica composite, are quite different to the one corresponding to Pr–

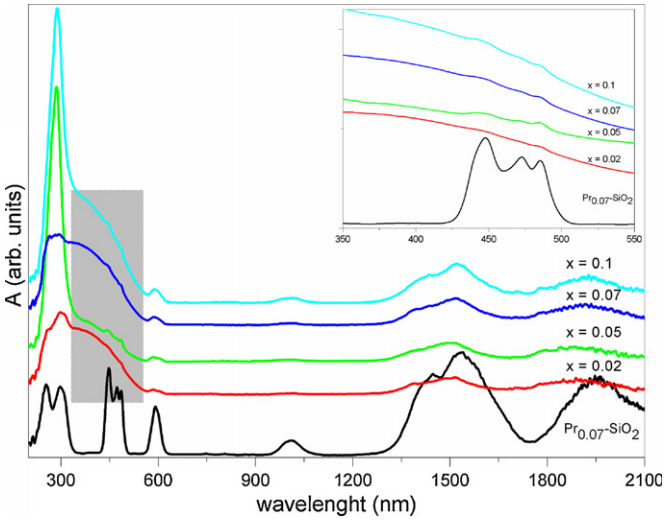

Fig. 4. DR spectra of gels Pr_x–$ZrSiO_4$ and $Pr_{0.07}$–SiO_2 annealed for 3 h at 1100 °C.

amorphous silica. The DR spectra of crystalline tetragonal zirconia–amorphous silica specimens display a narrow and strong band peaked at around 330 nm together with a strong absorption in the range between 350 and 590 nm and several weak bands centred at around 1500 and 1900 nm. In addition, three weak shoulders peaked at around 440, 470 and 485 nm and one additional weak band at around 600, are also detected. There are some recent reports on the reflectance spectra of Pr_x–ZrO_2 specimens prepared by the crystallization technique from nitrate salts, in which these bands have also been detected [19]. On the other hand, the spectrum of the Pr-containing silica is quite different, appearing a strong and wide band centred at around 380 nm and a series of absorption peaks, either single or set of peaks, in the regions of 440–510, 600, 1000, 1400–1500 and 1850–1950 nm, which have been attributed to the presence of Pr^{3+} cation [20,21].

From the above results it can be assumed that the location of Pr cation is associated with the zirconia phase, and even can be suggested that this incorporation of Pr occurred at the beginning of crystallization, i.e. at the stage in which nucleation of tetragonal ZrO_2 occurred during gel formation. Regarding to the oxidation state of Pr in the zirconia host lattice our results reveal that though in the spectra of samples with increasing amounts of praseodymium are detected very weak bands associated to the presence of Pr^{3+} it cannot be discarded the stabilization of Pr^{4+} in the zirconia host lattice probably associated with the wide absorption in the range between around 350 and 590 nm, shown as shaded in Fig. 4.

3.1.3. Structural changes from tetragonal Pr–ZrO_2 to Pr–$ZrSiO_4$ solid solutions

The transformation of Pr–ZrO_2(t) → Pr–ZrO_2(m) is a previous step to zircon formation in this pigmenting system. It is to note that the beginning of the zircon formation is always observed when that transformation is detected by XRD. The Pr location in the crystalline phase with monoclinic structure of ZrO_2 must be similar to the one in the prior tetragonal structure as evidenced by the DR spectra of specimens $Pr_{0.02}$–$ZrSiO_4$, $Pr_{0.05}$–$ZrSiO_4$, $Pr_{0.07}$–$ZrSiO_4$ and $Pr_{0.1}$–$ZrSiO_4$ annealed at 1300 °C/3 h, shown in Fig. 5. As shown in Fig. 3, the main crystalline phase present in those specimens display the monoclinic ZrO_2 structure. Both series of DR spectra of Pr–$ZrSiO_4$ specimens in Figs. 4 and 5 resemble similar appearance. From those results we can draw that monoclinic Pr–ZrO_2–amorphous silica composite can be quasi-selectively obtained by annealing Pr_x–$ZrSiO_4$ gel precursor at the required temperatures.

In Figs. 6 and 7 are shown the XRD patterns of gels annealed at 1450 °C for 3 h and 1600 °C for 24 h, respectively. It can be seen that as high temperature as 1450 °C, small amounts of both tetragonal and monoclinic Pr–ZrO_2 still remain unreacted for all compositions. The higher the nominal amount of Pr in the specimens the higher amount of unreacted Pr–ZrO_2. As it can be seen in Fig. 7 the formation of Pr-doped zircon final products can be considered to be complete at 1600 °C. However, very weak peaks corresponding to tetragonal Pr–ZrO_2 or monoclinic phases still remain in diffractograms. Also in specimens Pr_x–$ZrSiO_4$, with $x > 0.07$, can be detected $Pr_2Si_2O_7$ as secondary phase. The peak intensities of the silicate of praseodymium ($Pr_2Si_2O_7$, JCPD-732329) increases in the XRD patterns of specimens at 1600 °C on raising the nominal praseodymium loading.

It is interesting in this point some comments comparing the evolution from gels to zircon in Pr–$ZrSiO_4$ and V–$ZrSiO_4$

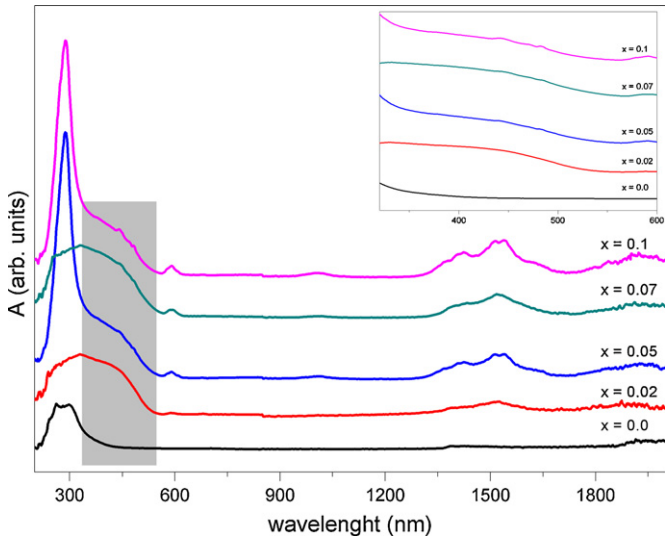

Fig. 5. DR spectra of gels Pr_x–$ZrSiO_4$ annealed for 3 h at 1300 °C.

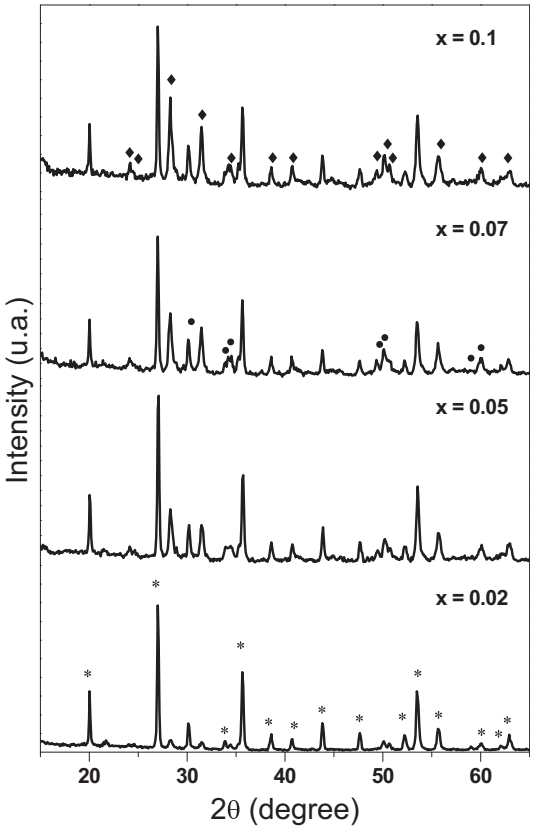

Fig. 6. X-ray diffraction patterns of gels Pr_x–$ZrSiO_4$ annealed at 1450 °C for 3 h (◆ is monoclinic zirconia, ● is tetragonal zirconia and * is zircon).

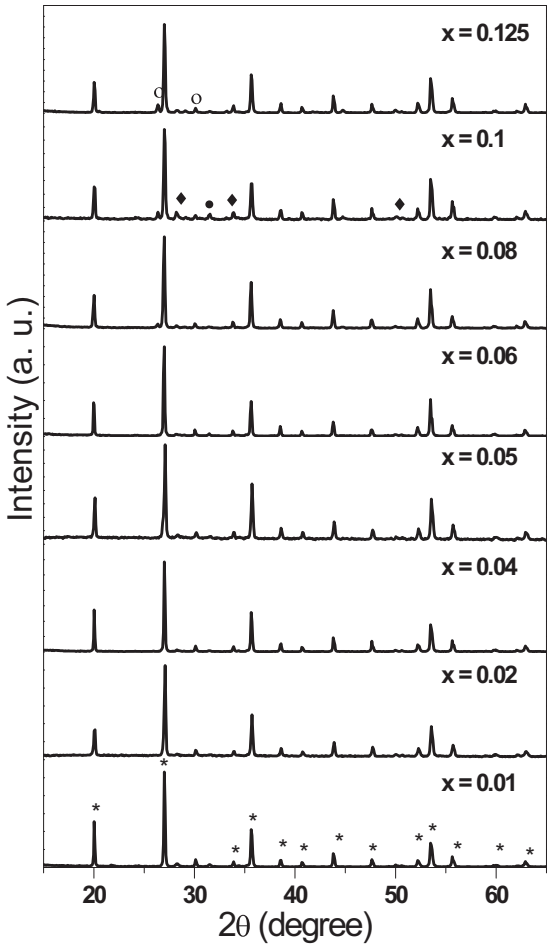

Fig. 7. X-ray diffraction patterns of gels Pr_x–$ZrSiO_4$ annealed at 1600 °C for 24 h (◆ is monoclinic zirconia, • is tetragonal zirconia, * is zircon and o is $Pr_2Si_2O_7$).

systems [12,13]. The whole process of zircon formation in both cases occurs through three steps. However, the stability on increasing the temperature of tetragonal and monoclinic V–ZrO_2 phases is very dependent on the vanadium nominal content in the V–zircon system. On increasing the vanadium loading the stability of both zirconia-based phases decreases, i.e. transform and/or react at lower temperatures. For Pr–zircon the stability of both phases based on polymorphs of ZrO_2 also depends on the Pr nominal amount but in the opposite direction. Thus, on increasing Pr content the Pr–ZrO_2 phases transform and/or react at higher temperatures.

3.2. Characterization of Pr–$ZrSiO_4$ solid solutions

In this section we intend to study some characteristics of the monophasic Pr–zircon solid solution products obtained at higher temperatures than 1400 °C. Thus, by establishing the relationship between lattice parameters and amount of Pr incorporated into the zircon phase in the series of annealed gels at 1600 °C, the simplest mechanism of solid solution formation and the limit of solubility can be inferred. Other outstanding features as the relative content of different oxidation states of Pr, specifically the 3+ and 4+, in the zircon structure will be also addressed.

Table 2
Lattice parameters of samples Pr_x–$ZrSiO_4$, annealed at 1600 °C/24 h.

x	c (Å)	V (Å^3)
0	5.9802(1)	260.710(1)
0.02	5.9794(1)	260.750(1)
0.05	5.9794(1)	260.780(1)
0.07	5.97971(1)	260.805(1)
0.1	5.9797(1)	260.810(1)
0.125	5.9793(1)	260.790(1)

3.2.1. Lattice parameters variation of Pr_x–$ZrSiO_4$ solid solutions

In order to determine changes in the unit cell of final Pr–zircon particulate products as a function of the Pr content inside the structure, the lattice parameters and the amount of Pr (as Pr_2O_3 wt%) incorporated into the zircon phase were experimentally determined. The lattice parameters and the composition (in wt%) for all specimens annealed at 1600 °C are shown in Tables 2 and 3, respectively. The differences in the content of praseodymium between both the whole and spot analysis are quite important for specimens with the higher praseodymium content. These results indicate the formation of a secondary phase rich in Pr ($Pr_2Si_2O_7$), already identified by XRD pattern. Furthermore, the above results also mean that for sample $P_{0.01}$–$ZrSiO_4$, the limit of solubility of praseodymium in zircon has been exceeded.

The variation in unit cell volume as a function of the praseodymium content entered into the zircon structure for specimens annealed at 1600 °C for 24 h is shown in Fig. 8. It can be seen (Table 2) that with increasing the Pr amount inside the phase with zircon structure, the parameters a and b rise and the parameter c keeps almost constant. The above changes in lattice volume bring about an expansion of the unit cell. This trend in lattice volume as the praseodymium content increases can be understood assuming the formation of a solid solution and is consistent with a simple mechanism of formation, by which the expansion of the unit cell is due to the replacement of a structural ion in the lattice by a larger one [22]. The zircon structure is described as chains of alternating edge-sharing tetrahedra SiO_4 and triangular dodecahedra ZrO_8 parallel to the c-axis which are joined laterally by edge-sharing dodecahedra [23]. The increase in lattice parameters a and b and also in lattice volume can be understood assuming that Pr is replacing Zr cations in dodecahedral sites of zircon structure. The

Table 3
SEM/EDX microanalysis results (wt%)[a] for samples annealed for 24 h at 1600 °C overall analysis spot analysis.

Sample	SiO_2	ZrO_2	Pr_2O_3	SiO_2	ZrO_2	Pr_2O_3
0	32.6(1)	67.3(1)	0.0	34.3(1)	65.7(1)	0.0
0.02	31.9(1)	65.1(1)	3.03(1)	32.7(1)	64.7(1)	2.5(5)
0.05	32.8(1)	62.9(1)	4.2(3)	31.9(2)	63.6(2)	4.4(5)
0.07	31.9(1)	60.9(1)	7.16(3)	32.1(2)	58.5(3)	9.3(5)
0.1	30.4(1)	57.7(1)	11.9(3)	32.4(1)	56.4(3)	11.5(4)
0.125	30.9(1)	55.7(1)	13.4(1)	34.4(2)	55.9(1)	11.2(5)

[a] Averaged at least over six analysis.

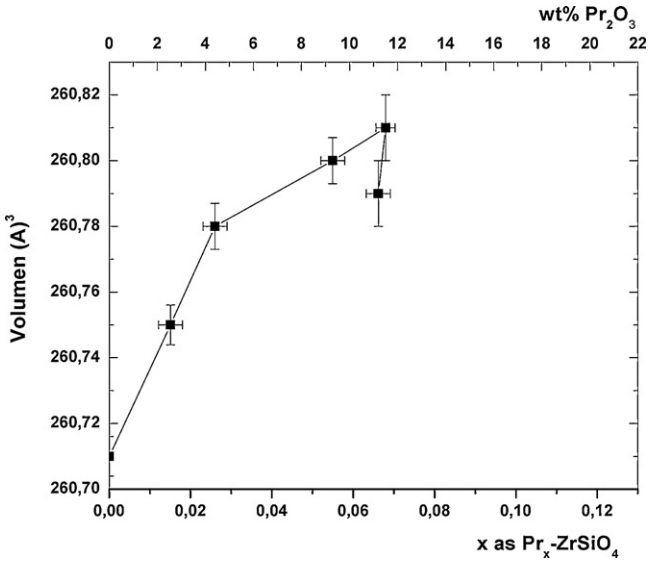

Fig. 8. Lattice volumes for Pr_x–$ZrSiO_4$ solid solutions as a function of praseodymium content.

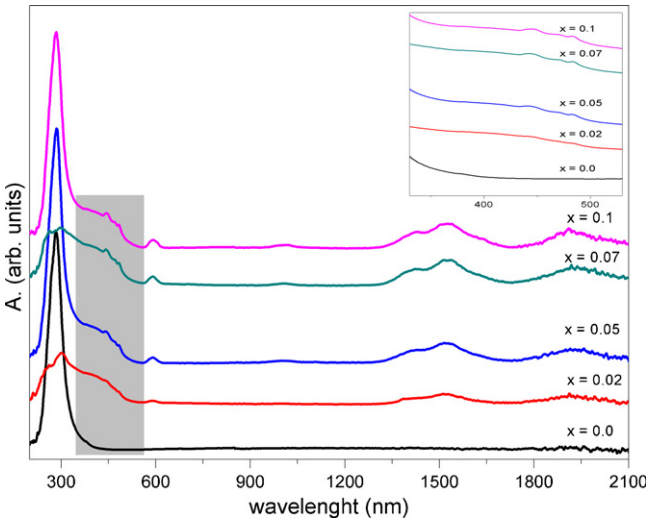

Fig. 9. Reflectance spectra of Pr^{4+}–$ZrSiO_4$ solid solutions heated at 1600 °C/24 h.

alternative mechanism involving the replacement of Si^{4+} by Pr in tetrahedral sites would also increase the lattice volume. However, that mechanism seems less probable because the difference in sizes of Pr (Pr^{4+} or Pr^{3+}) and Si^{4+} cations in tetrahedral coordination must be too large and the doped zircon phase would have low stability [22]. Thus, it can be assumed that the progressive increase of lattice volume on raising the amount of Pr inside the zircon structure is associated to the formation of solid solution phases with increasing amount of Pr replacing to Zr^{4+} cation. From the lattice volume changes it can be found the greater amount of Pr cation inside the zircon structure, i.e. the limit of solubility. From our results in Fig. 8, it can be seen the increase in the Pr-doped zircon lattice volume up to $x \approx 0.067$, which means that the solubility of Pr in the zircon structure is around 0.067 Pr mol per mol of zircon (~11.5 wt% as Pr_2O_3).

3.2.2. DR spectroscopy of Pr–$ZrSiO_4$ solid solutions

Diffuse reflectance spectra of Pr–zircon specimens with increasing contents of Pr annealed at 1600 °C for 24 h are shown in Fig. 9. In general, all spectra in the series of Pr-containing zircon samples are similar. As it can be seen single bands appear at 250, 440, 470, 485 and 600 nm as well as three sets of weak bands centred at around 1000, 1500 and 1950 nm. All these bands are associated with the presence of Pr^{3+} in oxidic lattices [19]. The strong band centred at around 250 nm shown by all specimens, including the undoped zircon, can be attributed to charge transfer transitions in the zircon lattice. However, recently Kempe et al. attributed this band to Pr^{4+}–O charge transfer [24].

Interestingly, an additional wide absorption between 330 and around 590 nm can also be seen in all the Pr_x–$ZrSiO_4$ samples. This absorption has been associated with the presence of Pr^{4+} in Mg- and Pr-codoped yttrium aluminium garnets, $Y_3Al_5O_{12}$ [25]. It is to note at this point the structural relation between the garnet and zircon structures [23]. The arrangement of tetrahedral and dodecahedral polyhedral are similar, being the main difference between both structures that octahedral sites in zircon are empty. This assignation is also supported by the similarity of absorption spectra of oxidic compounds containing either Ce^{3+} or Pr^{4+}, since both cations are isoelectronic, with electronic configuration f^1. Thus, results reported by Hamilton et al. on the absorption spectra of Ce^{3+}-doped yttrium aluminium garnet showed a set of $4f \rightarrow 5d$ transitions over the range 460–520 nm [26].

From the above experimental spectra can be assumed that even though the most part of the nominal amount of Pr is in the oxidation state (IV), a certain amount of Pr^{3+} is also present in the series of Pr–$ZrSiO_4$ solid solutions.

The evolution with praseodymium content of the $L^*a^*b^*$ parameters of samples heated at 1600 °C for 24 h in the series of samples, is shown in Table 4. Also, for the shake of comparison the colorimetric parameters of both a commercial praseodymium–zircon pigment and an undoped zircon are included.

In all Pr-doped zircon, those parameters correspond to a yellowish colour, the intensity of which increased on raising the praseodymium content up to the specimen $Pr_{0.06}$–$ZrSiO_4$. For

Table 4
$L^*a^*b^*$ parameters obtained for samples Pr_x–$ZrSiO_4$ annealed at 1600 °C temperatures for 24 h.

Sample	L^*	a^*	b^*
Commercial praseodymium-zircon	83.09	−0.14	51.75
$ZrSiO_4$	86.87	−0.43	0.2
$Pr_{0.02}$–$ZrSiO_4$	89.14	−3.17	12.09
$Pr_{0.04}$–$ZrSiO_4$	83.91	−5.50	18.74
$Pr_{0.05}$–$ZrSiO_4$	87.82	−4.26	16.26
$Pr_{0.06}$–$ZrSiO_4$	84.90	−7.03	25.03
$Pr_{0.07}$–$ZrSiO_4$	85.94	−3.99	16.82
$Pr_{0.08}$–$ZrSiO_4$	88.40	−6.29	18.57
$Pr_{0.1}$–$ZrSiO_4$	81.42	−3.91	16.43

larger praseodymium contents than $x = 0.06$, the parameter b^* lowers. An opposite trend was observed for the parameter a^*, whose minimum value was obtained for specimen $Pr_{0.06}$–$ZrSiO_4$.

4. Conclusions

Praseodymium–zircon gels obtained by chemical processing mixtures of zirconium n-propoxide, praseodymium acetylacetonate and tetraethylorthosilicate, were annealed at different temperatures up to the formation of zircon. The study by different experimental techniques allowed determining both the reaction sequence leading to Pr–zircon solid solutions and some structural and spectroscopic features of the reaction products. The results can be summarized as follows.

(a) Two transient crystalline phases, the first with tetragonal zirconia structure and the second with monoclinic one, both containing some amount of Pr are formed on heating gel precursors. The temperature of formation of tetragonal Pr–ZrO_2 solid solutions was independent on the amount of praseodymium in the starting gel. As the praseodymium oxide loading increased the Pr–ZrO_2 phases transformed or reacted at higher temperatures.
(b) The formation of Pr–$ZrSiO_4$ solid solution occurred by the reaction between the monoclinic form of Pr–ZrO_2 solid solution and the amorphous silica phase.
(c) The cell parameter variation as a function of praseodymium dissolved in $ZrSiO_4$ was consistent with the replacement of Zr by Pr in the zircon structure. The solubility of Pr into the $ZrSiO_4$ lattice was about 0.067 mol of Pr per mol of zircon ($\sim$11.5 wt% as Pr_2O_3).
(d) DR spectroscopy revealed that the main oxidation state of Pr in zircon was (IV) but a relatively small amount of Pr^{3+} was also present in all specimens.
(e) This study opens new perspectives to the development of more ecological zircon-based ceramic pigmenting systems by using mineralizer-free sol–gel techniques.

Acknowledgments

G. Herrera thanks CONACyT for a postdoctoral fellowship Grant No. 129569. Financial support from the MICINN (Ministry of Science and Innovation) through the CONSOLIDER-INGENIO 2010 program to the project CDS2010-00065 is acknowledged.

References

[1] R.A. Eppler, Zirconia-based colors for ceramic glazes, Am. Ceram. Soc. Bull. 56 (2) (1977) 213–218.
[2] C.A. Seabrigth, H.C. Draker, Ceramic stains from zirconium and vanadium oxides, Ceram. Bull. 40 (1961) 1–4.
[3] F.T. Booth, G.N. Peel, The principles of glaze opacification with zirconium silicate, Trans. Br. Ceram. Soc. 58 (1959) 532–564.
[4] M. Shoyama, H. Nasu, K. Kamiya, Preparation of rare earth–zircon pigments by the sol–gel method, J. Ceram. Soc. Jpn. Int. Ed. 106 (3) (1998) 274–289.
[5] M. Ocaña, A. Caballero, A.R. Gonzalez-Elipe, P. Tartaj, C.J. Serna, Valence and localization of praseodymium in Pr-doped zircon, J. Solid State Chem. 139 (2) (1998) 412–415.
[6] M. Ocaña, A. Caballero, A.R. Gonzalez-Elipe, P. Tartaj, C.J. Serna, R.I. Merino, The effects of the Naf Flux on the oxidation state and localisation of Praseodymium in Pr-doped zircon pigments, J. Eur. Ceram. Soc. 19 (5) (1999) 641–648.
[7] J.A. Badenes, J.B. Vicent, M. Llusar, M.A. Tena, G. Monrós, The nature of Pr–$ZrSiO_4$ yellow ceramic pigment, J. Mater. Sci. 37 (7) (2002) 1413–1420.
[8] G. Del Nero, G. Cappelletti, S. Ardizzone, P. Fermo, S. Gilardoni, Yellow Pr–zircon pigments: the role of praseodymium and of the mineralizer, J. Eur. Ceram. Soc. 24 (14) (2004) 3603–3611.
[9] J.K. Kar, R. Stevens, C.R. Bowen, Processing and characterisation of Pr–zircon pigment powder, Adv. Appl. Ceram. 104 (5) (2005) 233–238.
[10] A. Doménech, J. Alarcón, Vanadium-doped zircon and zirconia materials prepared from gel precursors as site-selective electrochemical sensors, Instrum. Sci. Technol. 31 (2) (2003) 121–140.
[11] A. Doménech, F.J. Torres, J. Alarcón, Electrochemistry of vanadium-doped $ZrSiO_4$. Site-selective electrocatalytic effect on nitrite oxidation, Electrochim. Acta 49 (26) (2004) 4623–4632.
[12] C. Valentín, M.A.C. Muñoz, J. Alarcón, Synthesis and characterization of vanadium-containing $ZrSiO_4$ solid solutions from gels, J. Sol–Gel Sci. Tech. 15 (3) (1999) 221–230.
[13] J. Alarcón, Crystallization behaviour and microstructural development in $ZrSiO_4$ and V–$ZrSiO_4$ solid solutions from colloidal gels, J. Eur. Ceram. Soc. 20 (11) (2000) 1749–1758.
[14] A.K. Varshneya, N. Suh, Sol–Gel-derived soda-lime-high-silica glass, J. Am. Ceram. Soc. 70 (1) (1987) C21–C22.
[15] C.J. Brinker, D.M. Haaland, Oxynitride glass-formation from gels, J. Am. Ceram. Soc. 66 (11) (1983) 758–765.
[16] M. Nogami, Glass preparation of the ZrO_2–SiO_2 system by the sol–gel process from metal alkoxides, J. Non-Cryst. Solids 69 (2–3) (1985) 415–423.
[17] K. Ishida, K. Hirota, O. Yamaguchi, H. Kume, S. Inamura, H. Miyamoto, Formation of zirconia solid-solutions containing alumina prepared by new preparation method, J. Am. Ceram. Soc. 77 (5) (1994) 1391–1395.
[18] A. Bertoluzza, C. Fagnano, M.A. Morelli, V. Gottardi, M. Guglielmi, Raman and infrared-spectra on silica–gel evolving toward glass, J. Non-Cryst. Solids 48 (1) (1982) 117–128.
[19] F. Ramos-Brito, C. Alejo-Armenta, M. García-Hipólito, E. Camarillo, J.A. Hernandez, H.S. Murrieta, C. Falcony, Photoluminescent emission of Pr^{3+} ions in different zirconia crystalline forms, Opt. Mater. 30 (12) (2008) 1840–1847.
[20] G. De, A. Licciulli, M. Nacucchi, Uniformly dispersed Pr^{3+} doped silica by the sol–gel process, J. Non-Cryst. Solids 201 (1996) 153–158.
[21] A. Biswas, H.N. Acharya, Pr^{3+} activated silica phosphor glasses by sol–gel method, Mater. Res. Bull. 32 (11) (1997) 1551–1557.
[22] R.D. Shannon, C.T. Prewitt, Revised values of effective ionic radii, Acta Cryst. B26 (1970) 1046–1048.
[23] K. Robinson, G.V. Gibbs, P.H. Ribbe, The structure of zircon: a comparison with garnet, Am. Miner. 56 (1971) 782–790.
[24] U. Kempe, S.M. Thomas, G. Geipel, R. Thomas, M. Plötze, R. Böttcher, G. Grambole, J. Hoentsch, M. Trinkler, Optical absorption, luminescence, and electron paramagnetic resonance (EPR) spectroscopy of crystalline to metamict zircon: evidence for formation of uranyl, manganese, and other optically active centers, Am. Miner. 95 (2010) 335–347.
[25] D. Pavlak, Z. Frukacz, Z. Mierczyk, A. Suchocki, J. Zachara, Spectroscopic and crystallographic studies of YAG:Pr^{4+} single crystals, J. Alloys Compd. 275/277 (1998) 361–364.
[26] D.S. Hamilton, S.K. Gayen, G.J. Pogatshnik, R.D. Ghen, W.J. Miniscalco, Optical-absorption and photoionization measurements from the excited states of Ce^{3+}:$Y_3Al_5O_{12}$, Phys. Rev. B 39 (13) (1989) 8807–8815.